

## Investigation of Damage and Fracture Properties of a Ring Cut from Filament-Wound Pipes with and without Delamination

A.M.Ahmad Zaidi <sup>1,\*</sup>, H.Abdul Hamid <sup>2</sup>, N.H.Ahmad Zaidi<sup>3</sup>, A.F.Ahmad Zaidi <sup>4</sup> and M.S.Yusof <sup>1</sup>

<sup>1</sup> Faculty of Mechanical and Manufacturing Engineering, UTHM, Malaysia

<sup>2</sup> School of MACE, The University of Manchester, U.K

<sup>3</sup> School of Material Engineering, UniMAP, Malaysia

<sup>4</sup> School of Mechatronic Engineering, UniMAP, Malaysia

\*corresponding author: mujahid@uthm.edu.my

### *Abstract:*

The technological advances in various industries have increased the demands on new engineered material tremendously since conventional materials such as steel, failed to perform in severe conditions. Nowadays, composite materials especially fibre-reinforced plastic composites (FRP) are broadly being used in many engineering fields to manufacture critical components with high stress concentration, exposure to extreme surrounding or weight constraint. However, they often suffer from a characteristic weakness, i.e. they are prone to interlaminar damage, often in a form delamination. In order to assess the development and the consequences of such damage, interlaminar fracture properties are essential. In this study, the ring cut specimen from filament-wound pipes with and without delamination was modelled and simulated based on experimental work using finite element modelling to further assist the identification and determination of the fracture properties. Investigation also involves the effect of the delamination length to the Energy Release Rate,  $G$ . Comparison between 23mm delamination of simulation and experimental results from [7] is presented.

**Keywords:** fibre-reinforced plastic composites, finite element, energy release rate

### **1. Introduction**

Many structure components on aircraft, light-weighted amours for defence and pressure vessels for commercial usage are made of fibre-reinforced plastic composites (FRP). Furthermore, it is also extensively used in piping system for oil industry, marine and commercially to transfer substance from one place to another and retain the longevity of life period of structure[1-3]. Most of these composites structures especially fibre-reinforced cylindrical components or pipes are produced by filament-winding technique simply because of its fast production time

and low cost compare to other alternative techniques[1-3].

Fibre reinforcements are the primary contributors of strength and stiffness of a composite structure. They work more efficiently when they are in bulk form because most of fibre material becomes stronger and stiffer in this form. Common material used to make these fibre reinforcements are brittle material such as glass, carbon and ceramic. Composite with fibre reinforcement have excellent tensile strength and stiffness in longitudinal or fibre direction but low mechanical properties in transverse direction and longitudinal

compression strength. This explains the anisotropic feature of a composite material which material properties vary in every direction of material.

Dominating the strength and stiffness in direction perpendicular to the fibre is matrix properties[1-3]. Matrix has weaker strength compare to fibre but it acts as the binder of all fibre reinforcements and provides the load distribute mechanism to the fibres implanted in the composite structure. Additionally, it functions to prevent the fibres from being exposed to corrosion, protect them from being damaged and contribute to material properties such as toughness and ductility. Polymeric, metallic, ceramic and carbon are the types of matrices used in composites which polymeric is the most common matrix used in producing filament wound pipes.

Filament wound pipes are constructed by stacking cylindrically a number of layers containing long and continuous fibres surrounded by matrix, in the direction of lamina thickness[1-2]. The material properties of these composites structure is mainly affected by the material of fibre and matrix, type and angle of fibre orientations and the stacking sequence of layers with different angle of fibre orientation. Since fibre reinforcement has tremendous strength in fibre direction, multidirectional-fibres laminates lay up is built to enhance the strength in all direction of composite structure. The main concern in laminate composite structure is the strength of bond between the layers which is mainly governed by matrix properties.

Composite with weak strength of matrix will results in poor interlaminar fracture toughness. When such composite is subjected to compressive loading, interlaminar damage will occur easily thus initiates the propagation of intralaminar matrix cracking transverse to the fibre and interlaminar delamination. Nevertheless, for

ring cut from filament wound pipe, when radial compressive loading is applied, interlaminar delamination is the major form of failure that is most likely to occur therefore only this form of damage will be focused from this point on. Interlaminar delamination is the separation of adjacent laminae in the plane of laminae interface that cause by interlaminar stresses. The presence of delamination in filament wound pipe will redistribute the stress distribution over the whole model and affects the structural integrity when the delamination becomes decisive. For example, damage on composite pipes can lead leakage of fluids or burst of high-pressure pipes [4]. Thus, dangerous consequences could happen such as explosion if the high-pressure pipes transport flammable gases or water pollution to the sea if the oil transmitting pipe located at the sea base. These huge impacts of composite pipe damage demand that deep investigation has to be done on development and propagation of interlaminar delamination.

Previously, many researchers have carried out tests and models experimentally and computationally to investigate the interlaminar fracture properties of composite structure[4-6]. Till today, there is no efficient and simple method to obtain the exact value of fracture properties because they may not be constant material properties but may also have to depend on the layer (fibre) orientation and the laminate stacking sequence [1]. Consequently, most of the previous researchers have agreed that fracture mechanics should be used to investigate the propagation of delamination. The same concept is also adopting in [7]. In his work, some experimental tests have been performed on ring cuts from filament wound pipes made of S-glass fibre and epoxy resin with anti-symmetry sequence of  $55^\circ$  and  $-55^\circ$  angle of fibre orientation. In this study, the interlaminar fracture is further investigated using finite element modelling

with the same properties and test specimens in [7].

## 2. Theory in Finite Element Modelling

### 2.1 Minimum Potential Energy

The fundamental concept of FEM in strain or displacement analysis is Minimum Potential Energy Concept which can be shown on axially loading on a bar with constant cross-sectional area. The relation of Minimum Potential Energy for all elements on the FEM model is described below [8], i.e.

$$\frac{\delta\pi}{\delta\{U\}} = \left( \sum_{e=1}^E [k^{(e)}] \right) \{U\} - \{F\} = 0 \quad (1)$$

Where  $\left( \sum_{e=1}^E [k^{(e)}] \right)$  is Global Stiffness Matrix,

$\{U\}$  is Displacement Vector, and  $\{F\}$  is Applied Force.

### 2.2 J-Integral Calculation

J-Integral is defined as the energy release rate of crack advance in a model. For a Virtual Crack Advance,  $\lambda$  (s), in three-dimensional plane of fracture, the Energy Release Rate is given by [8]:

$$\bar{J} = \int_A \lambda(s) n \cdot H \cdot q \, dA \quad (2)$$

Where  $\lambda$  (s) is Virtual Crack Advance,  $dA$  is surface element along a vanishing small tubular surface enclosing the crack tip or crack line,  $n$  is outward normal to  $dA$ ,  $q$  is the local direction of virtual crack advance and  $H$  is given by,

$$H = \left( WI - \sigma \cdot \frac{\partial u}{\partial x} \right) \quad (3)$$

Where  $W$  is elastic strain energy for elastic material.

Ideally, J-Integral should be domain independent provided that crack faces on the model are parallel to each other. However, in the simulation model, due to approximation of finite element solution, estimation of J-Integral varies from one ring of contour to another with crack tip as the centre of the

contour. Strong variation these estimations indicates that there is domain dependency or contour dependency of J-Integral which commonly denotes that an error has occur in defining contour integral. While, finer mesh is needed if gradual deviation in J-Integral estimations is obtained.

## 3. Model Development

Basically the simulation model is developed based on experimental work done by [7]. The material properties and the geometry information for the simulation model is based on [7], as shown in Table 1, Table 2 and Figure 1.

Table 1: Material descriptions

| Title                      | Description          |
|----------------------------|----------------------|
| Material of fiber          | E-glass              |
| Type of fiber              | Long and continuous  |
| Type of composite          | Laminates            |
| Material of matrix         | Epoxy                |
| Angle of fiber orientation | $\pm 55^\circ$       |
| Stacking sequence          | Anti-symmetric plies |
| Number of ply              | 8                    |

Table 2: Material properties

| Title                                    | Description         |
|--|---------------------|
| Longitudinal Young's Modulus, $E_1$      | $45 \times 10^9$ Pa |
| Transverse Young's Modulus, $E_2$        | $15 \times 10^9$ Pa |
| Out-of-plane Young's Modulus, $E_3$      | $15 \times 10^9$ Pa |
| In-plane Poisson's Ratio, $\nu_{12}$     | 0.28                |
| Out-of-plane Poisson's Ratio, $\nu_{13}$ | 0.28                |
| Out-of-plane Poisson's Ratio, $\nu_{23}$ | 0.50                |
| In-plane Shear Modulus, $G_{12}$         | $5 \times 10^9$ Pa  |
| Out-of-plane Shear Modulus, $G_{13}$     | $5 \times 10^9$ Pa  |
| Out-of-plane Shear Modulus, $G_{23}$     | $5 \times 10^9$ Pa  |

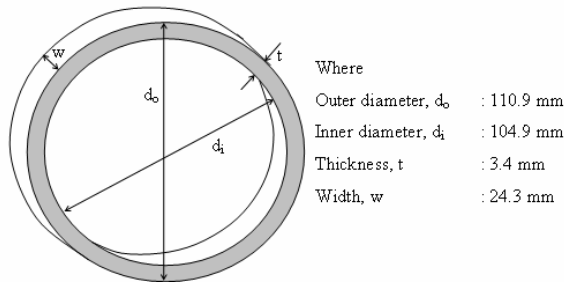


Figure 1: Specimen geometry

Due to symmetry of the specimen shape, loading and boundary conditions, only half of the ring geometry is modeled using 8-node bi-quadratic plane stress quadrilateral, reduced integration (CPS8R) element type and the loading and boundary conditions are similarly with the experimental work in[7].

### 3.1 Crack definition in simulation model

The crack is defined as illustrated in bold line in Figure 2(b) which propagates along the mid plane of ring thickness. The direction of crack propagation,  $q$  is defined using  $q$ -vector method[8] by selecting the start and end points of crack extension. The selected direction is indicated by the red arrow in Figure 2(a).

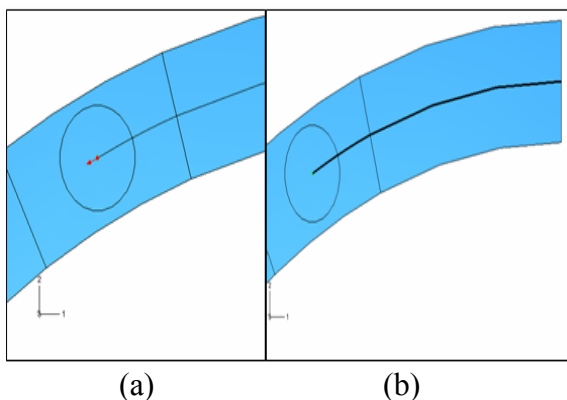


Figure 2: (a) Direction of crack propagation, (b) Crack line

## 4. Results and Discussions

### 4.1 Comparison of computational results between ring cut with delamination and without delamination

The presence of delamination in ring specimen redistribute the stress distribution around the ring specimen is shows in comparison between Figure 3 and Figure 4.

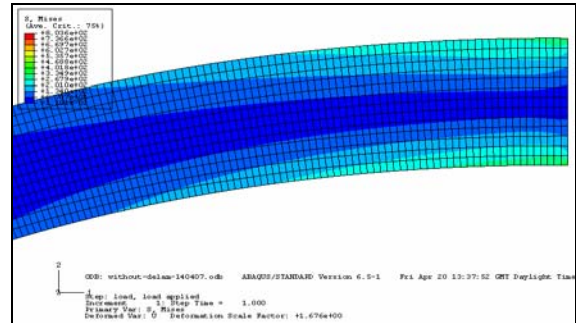


Figure 3: Stress distribution on upper part of ring specimen without delamination

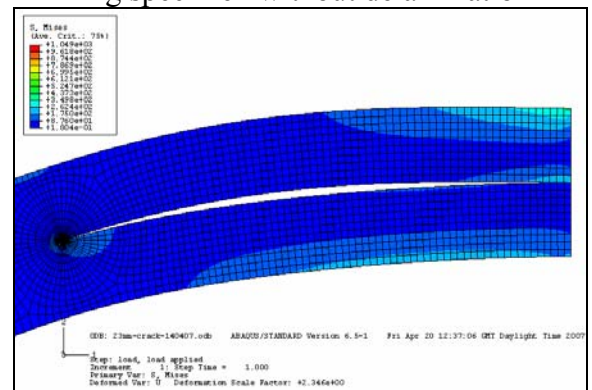


Figure 4: Stress distribution on upper part of ring specimen with 23mm delamination length

For ring without delamination, highest stress regions are located at upper surface and bottom surface of top of the ring region and reducing towards the mid plane of ring thickness. This stress distribution is because the upper surface region experienced compression force while the bottom surface experienced tension force. However, for ring with delamination, along the ring thickness, there is a discontinuity of stress distribution at the crack line which forms two separate beams with different

stress distribution. The upper beam has the same stress distribution as explained above but the lower beam has low stress region on top. The explanation for this is because there is no direct stress applied on top of the bottom beam or in other words on the delamination surface. The bottom surface of the lower beam still has high stress region due to tensile stress.

Opening or separation at the delamination area indicates that in this test, delamination mode is not only contributed by Shearing Mode (Mode II) but also could cause by Opening Mode (Mode I). Maximum stress seems to occur at the crack tip of delamination which is indicated by red color region in Figure 5. This outcome agrees with the prediction where as the load applied increases until a sufficient amount, delamination propagation starts at this point.

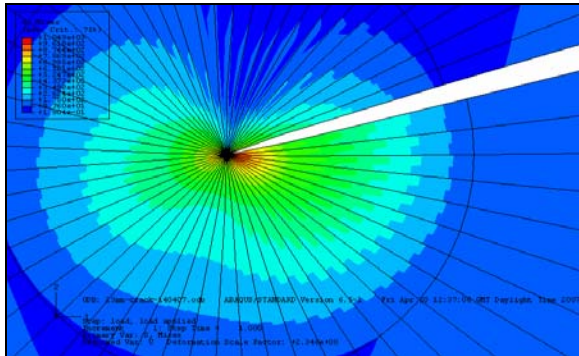


Figure 5: Stress distribution around crack tip of ring specimen with 23mm delamination length

#### 4.2 Comparison of computational results between different delamination lengths

The comparison between different delamination lengths is shown in Figure 6 for the 5mm and 7mm loading displacement.

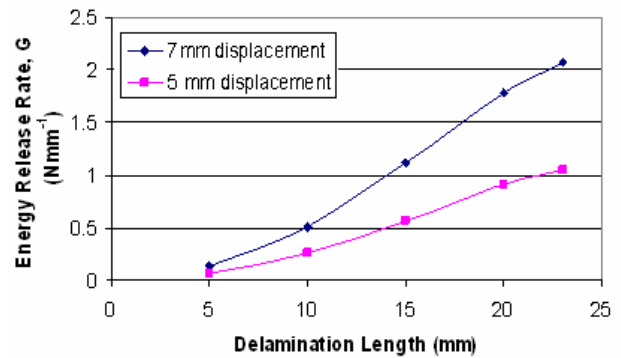


Figure 6: Graph of Energy Release Rate, G against Delamination Length

It shows that the Energy Release Rate, G is proportional to delamination length where theoretically [2], as delamination length increases, the Energy Release Rate, G should become smaller. This contradiction is most probably caused by the instability of the delamination propagation. In unstable delamination propagation, as Energy Release Rate, G reached the Critical Energy Release Rate,  $G_c$ , the delamination propagates even though the load displacement remains constant. Also, Energy Release Rate, G increases as delamination extends. Conversely, in a stable delamination extension, as delamination length increases, Energy Release Rate, G increases until it reaches Critical Energy Release Rate,  $G_c$  for the delamination starts to propagate. Then, as load increases further, delamination extends and the Energy Release Rate, G decreases. The same relationship between G and delamination length is obtained for 5mm and 7mm loading displacement.

#### 4.3 Comparison of computational results and experimental results

Comparison between simulation and experimental results shows that the Energy Release Rate, G obtained from simulation model is slightly close to the experimental result, which at 7mm loading displacement

and 46mm delamination length (23mm for half ring model), simulation results gives Energy Release Rate,  $G$  of  $2.068 \text{ Nmm}^{-1}$  while experimental results from [7] gives  $2.126 \text{ Nmm}^{-1}$ .

## 5. Conclusion

Based on the simulation results, it can be concludes that the existence of delamination damage in the composite laminated ring-cut will rearrange the stress distribution over the ring specimen and highest stress concentration area is located at the crack tip. Also, for instable delamination propagation, as the delamination length increases, the Energy Release Rate,  $G$  of the ring structure increases. Encouraging prediction is observed when simulation result is compared with experimental results[7].

**Acknowledgement:** The first and second authors would like to acknowledge the beneficial discussion with Dr.Z.Zou (The University of Manchester).

## References

- [1] I. M. Daniel, O. Ishai, *Engineering Mechanics of Composite Materials*, Oxford University Press, New York, USA 1994
- [2] B. Harris, *Engineering Composite Materials*, The Institute of Metals, England, UK1986.
- [3] D. Hull, T.W. Clyne, *An Introduction to Composite Materials*, Cambridge University Press, Cambridge, UK 1996
- [4] Z. Zou, S. R Reid, S. Li, P. D. Soden, *Composite Structures*, 56, pp.375-389, 2002.
- [5] N. aral, H. Gueznoc, P. Davies, C. Baley, *Materials Letters*, 62, pp. 1069-1099, 2008.
- [6] M. Arai, Y. Noro, K.I. Sugimoto, M. Endo, *Composites Science and Technology*, 68, pp.516-525, 2008.
- [7] Kwok Jin Hong, *Test Procedure and Measurement of the Critical Energy Release*

*Rate,  $G_{IC}$  of GRP Pipes*, Third Year Project Report, School of MACE, The University of Manchester, 2004.

[8] ABAQUS User's Manual Volume II Version 6.5, ABAQUS Inc. 2004, PDF format.